# Investigation of metallurgical phenomena related to process and product development by means of High Temperature Confocal Scanning Laser Microscopy

IOP Conf. Series: Materials Science and Engineering **119** (2016) 012003 doi:10.1088/1757-899X/119/1/012003

# Investigation of metallurgical phenomena related to process and product development by means of High Temperature Confocal Scanning Laser Microscopy

**U Diéguez-Salgado[1], S Michelic[1] and C Bernhard[1]**

[1]Chair of Ferrous Metallurgy, Montanuniversitaet Leoben, Franz Josef Straße 18, 8700 Leoben, Austria

E-Mail: Uxia.Dieguez-Salgado@unileoben.ac.at

**Abstract**. An increased interest for high temperature metallurgical processes appeared during the last decades, in order to achieve the high quality requirements in steel products. A defined steel cleanness and microstructure essentially influence the final product quality. The high temperatures involved in metallurgical processes and the lack of in situ observations do not only complicate the verification of simulation model predictions but also make significant conclusions regarding the industrial processes difficult. For that reason, new tools and techniques are necessary to develop. By combining the advances of a laser, confocal optics and an infrared image furnace, the High Temperature Confocal Scanning Laser Microscopy (HTCSLM) is a strong tool which enables high temperature in situ observations of different metallurgical phenomena. Next to solidification processes and phase transformations also the behavior of inclusions at different interfaces in the system steel-slag-refractory can be observed. The present study focuses on the aspects of inclusion agglomeration in the liquid steel and the inclusion behavior at the steel/refractory interface in two different steel grades. Out of the obtained experimental data, attraction forces are calculated and compared. This information provides an important basis for a better understanding of inclusion behavior in industrial processes and the therewith related process optimization, like for example the clogging phenomenon during continuous casting.

## 1. Introduction

The final quality of a steel product is always closely connected to its metallurgical production process. Different possibilities and procedures during secondary metallurgy as well as during continuous casting exist in order to ensure the demands of customers regarding mechanical properties, corrosion resistance and surface quality. A parameter which significantly influences steel quality is the so called steel cleanness. The latter is defined through the number, size, chemical composition, distribution and morphology of non-metallic inclusions in the steel matrix. Due to the necessity of deoxidation, the formation of inclusions cannot be avoided completely. In order to ensure a possibly low content of inclusions in the steel and to enable a specific inclusion modification, their behavior in the system steel-slag-refractory needs to be well understood.

Figure 1 gives an overview on possible reactions and interactions of inclusions at different interfaces. Non-metallic inclusions collide and agglomerate in the liquid steel in order to form larger particles; if

the particles are large enough, they are transported by flotation to the liquid steel/slag interface due to the density difference between the liquid steel and inclusion, by bubble attachment or by fluid transport in the metallurgical vessel and removed from the steel to the slag by dissolution. Some small inclusions could be transported to the liquid steel/refractory interface and adhering to the wall refractory and others could stay suspended in the liquid steel and pass onto the next stage of the steelmaking process. [1,2]

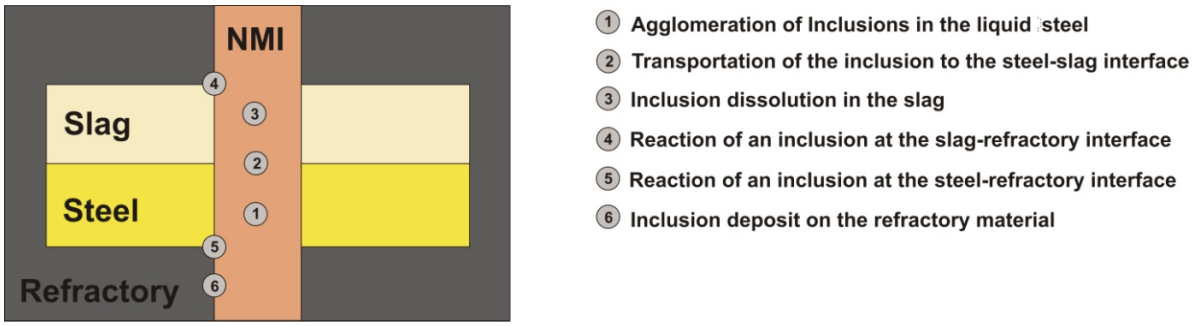


**Figure 1.** Overview on possible reaction sites in the system steel-slag–refractory.

The present study gives an insight in the possibilities of in-situ observation concerning the behavior of non-metallic inclusions at different interfaces between steel, slag and refractory material and indicates the practical relevance for process and therefore product improvements in steelmaking.

## 2. Theoretical background

In the continuous casting process, the submerged entry nozzle (SEN), plays a vital role in order to ensure stable casting conditions. The clogging phenomenon – characterized by a substantial reduction of the inner section of the nozzle caused by material build up – can lead to a disruption of normal casting operations and also produces an uneven flow of molten steel in the mold, finally leading to the formation of inclusion clusters which deteriorate the product quality. The agglomerates found in the nozzle often primarily consist of $Al_2O_3$ particles. [3–8] Next to the principal source of particles [9] causing clogging, the adhesion between particles and the refractory material as well as the attraction between two particles are points of interest.

### *2.1 Adhesion between non-metallic inclusions and liquid steel*

Several research groups dealt with this phenomenon in the past. Singh [7,10–12] divided the deposition process into three stages: (i) The particles are transported from the bulk melt to the refractory surface and come in contact with the nozzle refractory (ii) The inclusions adhere to the refractory surface and (iii) inclusions adhere to each other and sinter together to form a network. The characteristics of the system liquid steel/refractory, such as wettability, composition and surface tension will significantly influence the attachment step.

Sasai et al. [13,14] conclude in their investigation that the agglomeration force between alumina particles in Al deoxidized molten steel is not caused by the van der Waals force but the cavity bridge force created due to the fact that alumina particles are unlikely to be wetted by molten steel. In non-wetting conditions, when two spherical non-metallic inclusions/particles of radii $r_1$ and $r_2$ approach, the steel in contact area may be expelled, leaving an empty neck (filled with gases and vapours) of concave lens shape. The adhesion force is bigger than the buoyancy force and also the flow resistance that acts on the particles, so that the particles will remain at the interface. [10,11,13–15]

This attractive force is the sum of the surface tension force and the force that results from the pressure drop across the liquid-gas interface. [13,15] The balance of forces can be written as follows (The force balance is calculated in the thinnest point of the neck):

$$F_{adh} = 2\pi R_2 \sigma + \pi R_2^2 \Delta P \quad (1)$$

where σ= surface tension of molten steel, ΔP= difference pressure and $R_2$ = Curvature radius (geometrical parameter) [10,11,13–16]

Applying Equation 1, Figure 2 is calculated. The attraction force is estimated assuming the case that non-metallic inclusions (radii 2,5µm) attach to different refractory walls at the melt depth of 1 m and with 1,8N/m surface tension of molten steel. Three different situations are plotted in Figure 2:

1) The adhesion force between alumina particles and an alumina refractory wall.
2) The adhesion force between alumina particles and a zirconia refractory wall.
3) The adhesion force between liquid calcium aluminate inclusions, from Ca-treated steel, and an alumina refractory wall.

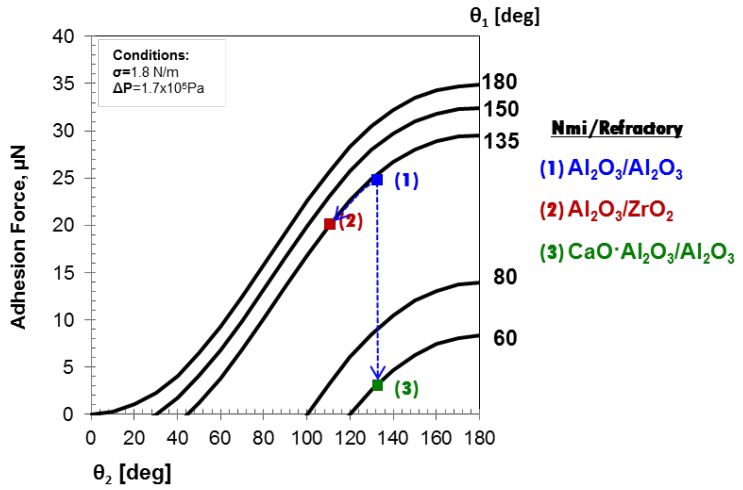


**Figure 2.** Relation between the contact angles and adhesion force. ($\theta_1$ is the contact angle of the non-metallic inclusions with the molten steel and $\theta_2$ is the contact angle of the refractory material with molten steel, the value of the contact angles used are found in [17]).

The adhesion force between alumina non-metallic inclusions and an alumina refractory wall amounts to 25µN (1).

a) The decrease of the contact angle between the molten steel and the refractory leads to a lower adhesion force (2). However, according to a work by Eustatopoulos [5,18], it appears to be impossible to find a refractory-nozzle material with a low contact angle (below 60°-40°) and coincident low reactivity.
b) Assuming a particle from liquid calcium-aluminate instead of solid alumina results in a decrease of the contact angle between the molten steel and the non-metallic inclusions and consequently a significant decrease of the adhesion force (3).

As described in Equation 1, the attraction force is influenced by surface tension of the molten steel, the difference pressure between the molten steel and the gas cavity and the ‘shape’ of the cavity which depends on the non-metallic inclusions size, morphology and the wetting behaviour.

### *2.2. Attraction between non-metallic inclusions*

The non-wettability behavior of the majority of non-metallic inclusions for liquid iron generates a deformation of the liquid surface, which is called meniscus. If two particles approach one-another, the meniscus in between them is further depressed or drawn downward. [19] This change, which is called capillary attraction, can lead to a difference of capillary pressure between the inside and the outside area of the pair, which will push the two bodies towards each other. [20] The capillary attraction is believed to be the source of the attraction between alumina inclusions at free surfaces and at the surface of gas bubbles inside the liquid steel melt. [19]

The strength of the capillary attraction force for inclusion particle pairs in molten steel, which was found to be much different for particles with different morphology, can be listed as follows in ascending order [21]: liquid/liquid pair < liquid/semi-liquid pair < semi-liquid/semi-liquid pair < liquid/solid pair < semi-liquid/solid pair and finally solid/solid pair as the strongest. The latter sequence is only valid if only the effect of the particle morphology is considered. But the attraction between particles is also strongly affected by other parameters like for example by the particle size, the contact angle of a particle with steel melt, the particle density, the shape and the interfacial tension [22].

## 3. High Temperature Confocal Scanning Laser Microscopy (HT-CSLM)

By combining the advances of a laser, confocal optics and an infrared image furnace, the high temperature Confocal Scanning Laser Microscopy (HT-CSLM) is a strong tool which enables high temperature in situ observation of metallurgical phenomena as phase transformations in the steel [23,24] (e.g. the peritectic reaction or the nucleation of acicular ferrite), austenite grain growth [25], inclusion agglomeration in the liquid steel [26] or inclusion dissolution in a slag phase [27,28], as well as reactions at the steel/refractory interface. The obtained experimental data can be used for a quantitative evaluation of dissolution rates, attraction forces or diffusion coefficients.

The present work focusses on the in situ observation of non-metallic inclusions behavior at high temperature at liquid steel and liquid steel/refractory interfaces by means of High Temperature Confocal Scanning Laser Microscopy.

### *3.1. Set up.*

A Confocal Scanning Laser Microscope (VL2000DX from Lasertec) and a high temperature furnace (SVF17-SP from Yonekura) are used for all investigations. The decisive advantage of HT-CSLM in contrast to conventional microscopes or experimental facilities is the possibility of in-situ observations at temperatures up to 1700 °C in combination with a very good image quality. This is primarily possible due to the fact, that a laser is used as a light source. A schematic view of the experimental set-up in the high temperature furnace which shows an elliptic, gold coated inner contour as well as detailed configuration data of the set-up can be found elsewhere [29]. The halogen lamp is situated in the bottom focal point of the furnace. The sample holder with the crucible and sample inside is located in the top focal point of the ellipse. The temperature is measured with a thermocouple fixed at the bottom side of the sample holder. High-purity argon with a flow rate of 150 $cm^3$/min ensures a neutral atmosphere in the furnace. Additionally, the oxygen content in the furnace is measured for every experiment.

### *3.2. Experimental procedure.*

Two different experiments are performed:

- Inclusion agglomeration in the liquid steel: a steel disc with approximately 600µm thickness is placed in an $Al_2O_3$ crucible and subsequently set up on the sample holder in the ellipsoidal furnace (see Figure 3(a)). The specimen is heated up following the heating cycle given in Figure 4. An alumina disc is placed under the steel disc in order to avoid the attachment of the steel disc onto the crucible. When the liquidus temperature of the steel is reached, inclusions are starting to emerge from the bulk to the steel surface and their agglomeration behavior can be studied. In the present study a Ca-treated steel and a ULC steel are used (composition given in Table 1) in order to investigate the effect of particle morphology into the agglomeration behavior.
- Inclusion behavior at the steel/refractory interface: An exogenous alumina particle (400µm ECD) is placed on the top of a steel disc with approximately 600µm thickness, which is placed in an $Al_2O_3$ crucible (see Figure 3(b)). An alumina disc is placed below the steel disc to avoid the steel sticking onto the crucible. The specimen is heated up following also the heating cycle given in Figure 4. When the liquidus temperature is reached, inclusions are starting to emerge from the bulk to the steel surface and their behavior at the steel/refractory interface is investigated. In the present study the behavior of nonmetallic inclusions at the interface between alumina and a Ca-treated steel (see composition in Table 1) is observed.

**Tabla 1.** Investigated steels [wt.-%].

| Steel | C | Si | Mn | Al | S | Ca |
|---|---|---|---|---|---|---|
| **Ca-treated** | 0.15 | 0.02 | 1.07 | 0.04 | 0.004 | 0.0012 |
| **ULC** | 0,002 | 0,001 | 0.074 | 0,020 | 0,008 | 0,000 |

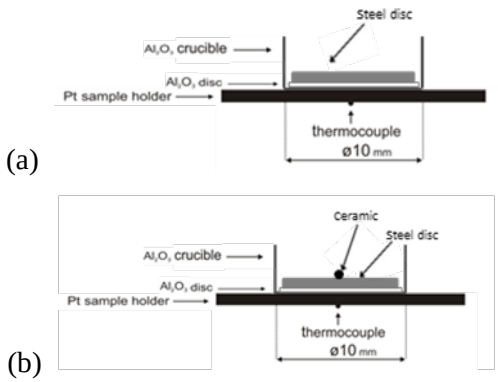


**Figure 3.** Experimental set up. (a) Inclusions agglomeration experiments. (b) Inclusion behavior at the steel/refractory interface.

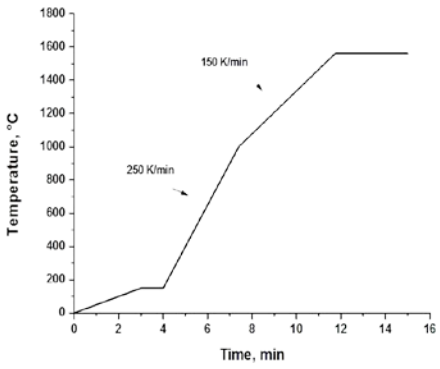


**Figure 4.** Time-temperature profile of the experiments.

A posteriori examination of the sample at room temperature is carried out using a Scanning Electron Microscope with Energy Dispersive XRays (SEM/EDS). In order to characterize (composition, shape, size) the inclusions observed during the experiment, a fast cooling of the sample is important [26].

For the quantitative evaluation of the experimental results, an approach of Yin et al. [20,21] is used. They described and compared the magnitude of the attraction force from measured acceleration of particles with a certain mass based on in-situ observations in the confocal microscope. The latter approach was also used of many other research groups. [12,19,30–32] Details about the evaluation procedure can be found in [20,26].

## 4. Results

*4.1. Inclusion agglomeration on the molten steel.*

Inclusion behavior in the liquid steel was studied in different steel grades (composition given in Table 1) also involving different inclusion types. Regarding the Ca-treated steel, results of inclusion agglomeration experiments and in-situ images displaying the inclusion movement and the subsequently calculated attraction forces have already been published previously [26]. It was found, that as soon as a large part of the sample surface melted, many inclusion particles emerged from the interior of molten steel bath and floated on the melt surface. The shape of the observed inclusions was mostly observed to be semi-liquid with irregular shape or liquid with globular shape.

Representative examples of detected inclusions analyzed in the SEM after the experiment and the corresponding chemical composition can also be found in a previous publication [26]. Generally, semi-liquid and liquid inclusions do not attract each other.

The contact angle of solid non-metallic inclusions and steel melt usually amounts to more than 90°. The capillary force decreases with decreasing contact angle and smaller density of the particle. The reduction of the contact angle and the density for liquid as well as semi-liquid particles results in smaller capillary forces compared with solid particles in agreement with [21]. Nevertheless, some interaction between the inclusions is observed close to the solidification front. The investigation of the trajectory path and the subsequent calculation of the attraction force for two semi-liquid inclusions showed that the tendency of agglomeration for liquid as well as for semi-liquid inclusions is smaller than for solid inclusions. According to literature [21] the attraction force between two of semi-liquid CA60 particles is approximately $10^{-16}$ -$10^{-15}$ N, which agrees well with results published previously [26].

In contrast, regarding the ULC steel, intense agglomeration, cluster formation and a large number of interactions between particles were observed during the whole experiment. A SEM-analysis of the inclusions after the in-situ experiments proved that solid, irregular shaped $Al_2O_3$ is the predominant inclusion type in this steel.

The experiments showed that alumina inclusions strongly attract to each other; the inclusions grow quickly by agglomeration which is again in good agreement Yin et al. [20,21].

From Figure 5, the calculated attraction force for two solid, irregular shaped alumina inclusion is in the range $10^{-14}$ -$10^{-15}$ N; for a pair of semi-irregular and semi-liquid inclusion the attraction force amounts to between $10^{-15}$ -$10^{-16}$ N. Therefore, the tendency of agglomeration for solid inclusions is higher than for the semi-liquid inclusions. This is again in good agreement with published by Yin et al. [21].

Possible explanations for these observed differences regarding the agglomeration tendency could be:

a) The wettability behavior: Solid inclusions are less wetted than liquid inclusions, this leads to a meniscus formation around the inclusions and therefore the capillary force appears.
b) The velocity of the inclusions: Liquid particles seem to move slower than solid ones and hence the calculated attraction force is lower.
c) The density of the particles.

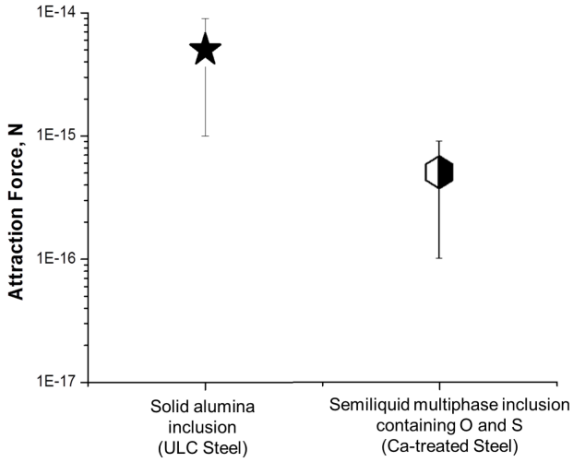


**Figure 5.** Comparison of attraction force between two same inclusion type for different composition/morphology and shapes.

*4.2. Inclusion behavior at the steel/refractory interface.*

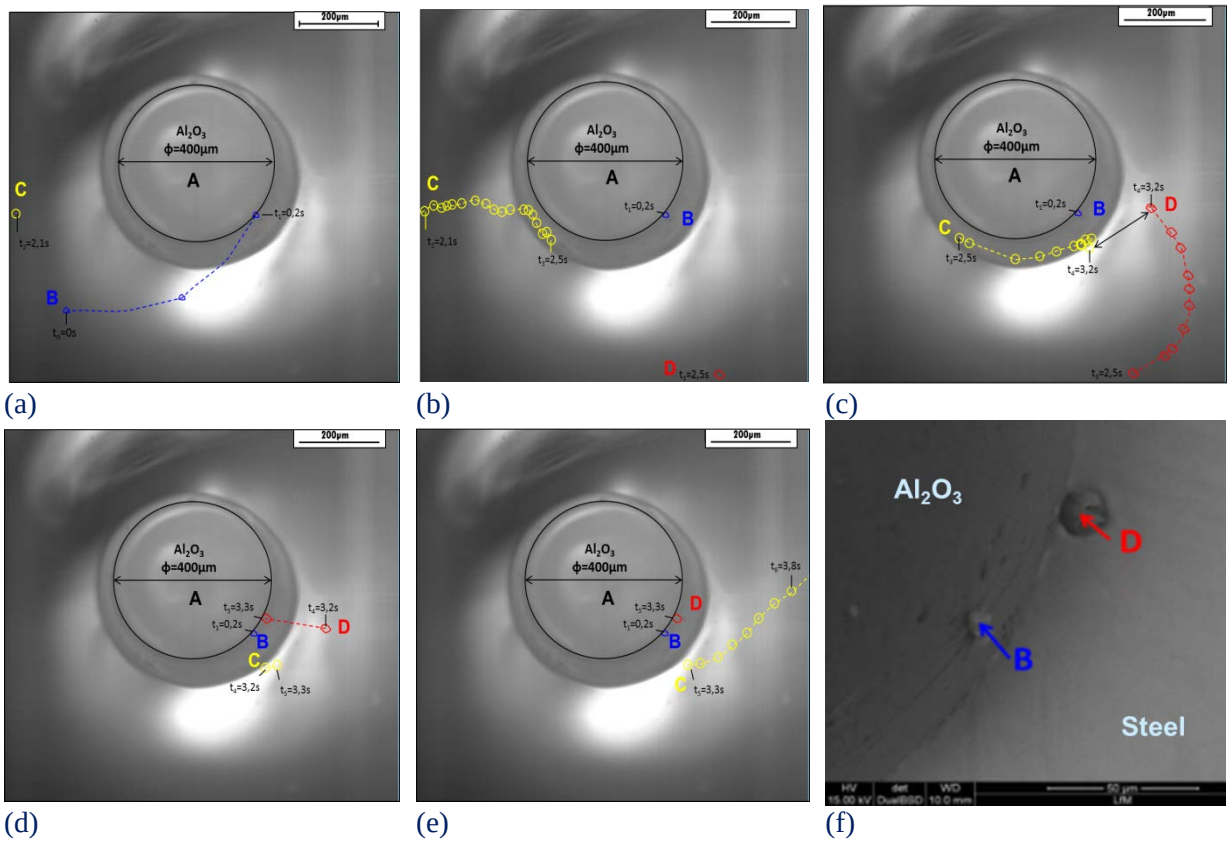


**Figure 6.** (a)-(e) Show the trajectory of three non-metallic inclusions B, C and D in relation to particle A. (f) SEM image.

In a first step, applying Equation 1, the attraction force is calculated modifying the size of one of the particles. The results show that for a 5µm ECD particle the attraction force is constant as soon as the

second particle is up to 100µm ECD. For this reason, a 400µm ECD alumina particle is placed on the top of a steel disc in order to observe the inclusions behavior at a flat refractory/steel surface.

From the agglomeration experiments with Ca-treated steel (see section 4.1) is observed that the tendency of agglomeration between semi-irregular semi-liquid inclusions is low. In this section, the behavior of the inclusions from Ca-treated steel at a liquid steel/alumina interface is investigated.

When the Ca-treated steel was melted around the alumina particle, some non-metallic inclusions float up. Different behavior of the particles in relation with the big alumina particle was observed. In Figure 6 (a) a particle B rapidly attaches to the large alumina particle (Particle A), after 2 seconds a globular particle C appears. The trajectory of particle C is observed (see Figure 6 (b)-(e)), it moves towards particle A, but instead of attaching, particle C keeps moving close to A and after some time, it moves away. In Figure 6 (b) a particle D is observed; after 0.8 seconds particle D attaches to A (see Figure 6 (c) and (d)). SEM-analysis of the inclusions after the in-situ experiments proved that inclusions B and D are attached to the alumina surface (See Figure 6 (f)).

The non-metallic inclusions B, C and D have different shapes. Globular particles like C are expected to be liquid and to show a low interaction at the steel/alumina interface as it is observed during the experiment, whereas B and D are semi-irregular semiliquid inclusions which show higher interaction at the steel/alumina interface.

The alumina sphere added to the experiment is non-wetted by the molten steel. The contact angle of B, C and D with the molten steel depends on the inclusions morphology and leads to different deformations of the liquid steel surface. During the experiments, it is observed that non wetting inclusions, like B and D, tend to attach to the alumina surface. However, the better wetted inclusions, like C, approach to the non-wetted surface but they don't attach.

The different morphology and wetting behavior of these non-metallic inclusions may be the cause of for the different behavior observed at the steel/alumina interface.

## 5. Conclusions

Based on the in-situ studies using Laser Scanning Confocal Microscopy the following conclusions regarding the behavior of non-metallic inclusions in the liquid steel and at the steel/refractory interface can be drawn:

- In general, the observation results confirm the common understanding that the wetting angle of liquid iron on non-metallic inclusions or on refractory materials is the dominating influencing factor for adhesion and agglomeration phenomena.
- For this reason, the tendency of agglomeration between solid inclusions (usually with a poor wettability for liquid iron) is higher than for semi-liquid inclusions (usually with a good wettability for liquid iron). Besides this, shape and density of particles are minor influencing parameters.
- The calculated attraction forces between the particles are in good agreement with literature.
- The same conditions apply to the behaviour of particles at refractory/steel interface.
- Future work will comprise the investigation of a wide number of different steel grades with their associated inclusion population in contact with commercial refractory materials for submerged entry nozzles and slide plates. The results will further on be validated in up-scaled, close-to-process experiments and finally help to specify criteria for the development of clogging inert refractory materials.

**Acknowledgements**

Financial support by the Austrian Federal Government and the Styrian Provincial Government, represented by Österreichische Forschungsförderungsgesellschaft mbH and by Steirische Wirtschaftsförderungsgesellschaft mbH within the research activities of the K2 Competence Centre on "Integrated Research in Materials, Processing and Product Engineering", operated by the Materials Center Leoben Forschung GmbH in the framework of the Austrian COMET Competence Centre Programme, is gratefully acknowledged.

**References**

[1] Braun T B, Elliott J F and Flemings M C 1979 *Metall. Trans. B* **10B** 171.
[2] Zhang L, Pluschkell W and Thomas B G 2002 *85th Steelmaking Conference* **85** 463.
[3] Rackers K G and Thomas B G 1995 *78th Steelmaking Conference* 723.
[4] V Vermeulen. B Coletti, B Blanpain, P Wollants and J Vleugels 2002 *ISIJ Int.* **42** 1234.
[5] Nadif M, Burty M, Soulard H, Boher M, Pusse C, Lehmann J and Meyer F 2004 *IISI Study on Clean Steel*.
[6] Wilson F G, Heeson M J and Rawson J D W 1988 *Technical Steel Research*.
[7] Singh S N 1974 *Metall.Trans.* **5** 2165.
[8] Ogibayashi S 1995 *Taikabutsu Overseas* **15**.
[9] Bernhard C, Xia G, Egger M, Pissenberger A and Michelic S 2012 *AISTech*.
[10] Uemura K, Takahashi M, Koyama S and Nitta M 1992 *ISIJ Int.* **32** 150.
[11] Kawecka-Cebula E, Kalicka Z and Wypartowicz J 2006 *Arch. of Metall. and Mater.* **51**.
[12] Aneziris C G, Schroeder C, Emmel M, Schmidt G, Heller H P and Berek H 2013 *Metall. Trans. B* **44B** 954.
[13] Sasai K 2014 *ISIJ Int.* **54** 2780.
[14] Sasai K and Mizukami Y 2001 *ISI Int.* **41** 1331.
[15] Zheng L, Malfliet A, Wollants P, Blanpain B and M Guo 2015 *ICS*.
[16] Mizoguchi T, Ueshima Y, Sugiyama M and Mizukami K 2013 *ISIJ Int.* **53** 639.
[17] Raiber K, Hammerschmid P and Janke D 1995 *ISIJ Int.* **35** 380.
[18] Eustathopoulos N and Drevet B 1994 *J. Phys. III* **4** 1985.
[19] Vantilt S, Coletti B, Blanpain B, Fransaer J, Wollants P and Sridhar S 2004 *ISIJ Int.* **44** 1.
[20] Yin H, Shibate H, Emi T and Suzuki M 1997 *ISIJ Int.* **37** 936.
[21] Yin H, Shibate H, Emi T and Suzuki M 1997 *ISIJ Int.* **37** 946.
[22] Nakajima K and Mizoguchi S 2001 *Metall. and Mater. Trans. B* **32B** 629.
[23] Loder D, Michelic S K and Bernhard C 2014 *MS&T*.
[24] Loder D, Michelic S K, Mayerhofer A, Bernhard C and Dippenaar R J 2014 *Junior Euromat*.
[25] Fuchs N, Krajewski P and Bernhard C 2015 *BHM* **160** 214.
[26] Michelic S K , Diéguez Salgado U and Bernhard C 2015 *LMPC* .
[27] Feichtinger S, Michelic S K, Kang Y, Bernhard C and Jantzen C 2014 *J. Am. Ceram. Soc.* **97** 316.
[28] Michelic S, Goriupp J, Feichtinger S, Kang Y, Bernhard C and Schenk J 2015 *Steel Research Int.* **86**.
[29] Bernhard C, Schider S, Sormann A, Xia G and Ilie S 2011 *BHM* **156** 161.
[30] Coletti B, Vantilt S, Blanpain B and Sridhar S 2003 *Metall. and Mater. Trans. B* **34 B** 533.
[31] Kimura S, Nakajima K and Mizoguchi S 2001 *Metall. and Mater. Trans. B* **32**.
[32] Wikström J, Nakajima K, Shibata H, Tilliander A and Jönsson P 2008 *I&S* **35** 589.